

Selected Papers

Dihedral Angle Dependence of Transfer Integrals in Organic Semiconductors with Herringbone Structures

Hirotaka Kojima* and Takehiko Mori

Department of Organic and Polymeric Materials, Tokyo Institute of Technology, O-okayama, Meguro-ku, Tokyo 152-8552

Received June 7, 2011; E-mail: kojima.h.ab@m.titech.ac.jp

The herringbone structure is a representative molecular packing in organic semiconductors, but there are some modifications with largely different dihedral angles ranging from 40 to 130°. Dihedral angle θ dependence of the transfer integrals is systematically investigated on the basis of the molecular orbital calculations for various organic semiconductors including pentacene, picene, oligothiophene, fused thiophene, tetrathiafulvalenes (TTF), and benzothienobenzothiophene (BTBT). In the conventional organic semiconductors such as pentacene and oligothiophene, the transfer integral is a monotonously decreasing function of θ starting from the stacking geometry, and smaller θ provides more two-dimensional bands. When the molecules are slipped along the molecular long axis D, these compounds show characteristic oscillating structure of the transfer integrals depending on D, which is called D-modulation. Contrarily, TTF derivatives show oscillating structure of the transfer integrals depending on θ (θ-modulation) due to interaction at the side position. BTBT exhibits a pattern much different from the conventional organic semiconductors, and a considerable magnitude of transfer integrals is expected in the large θ region. These systematic investigations demonstrate that the θ-dependence of the charge transport largely depends on the original molecular orbital symmetry.

Recently, considerable attention has been devoted to organic semiconductors due to large-area, flexibility, and easy-fabrication in organic electronics consisting of organic field-effect transistors (OFETs), organic light-emitting diodes, and organic photovoltaics.[1] It is characteristic of small-molecule organic semiconductors used in OFETs that highly ordered molecular packing is important for attaining high performance. Among the crystals of organic semiconductor molecules, the herringbone structure is a representative molecular arrangement. One of the most known examples is pentacene (Scheme 1a),[2] which has a largely inclined herringbone structure with a small dihedral angle of $\theta = 53°$ (Figure 1). Recently, it has been reported that OFET of picene shows high performance (Scheme 1c),[3] where $\theta = 58°$ is similar to pentacene.[4] Oligothiophene (Scheme 1d) is another representative of the herringbone structure, where θ is 50–60° (Figures 1d and 1e).[5] A very wide range of θ is, however, observed in other organic semiconductors (Figure 1); examples are 89° for perfluoropentacene (Scheme 1b and Figure 1b), which shows n-channel OFET characteristics, and 130° in pentathienoacene (f-5T, Scheme 1e, and Figure 1f).[6,7] Dibenzotetrathiafulvalene (DBTTF, Scheme 1g) is an OFET material investigated by many research groups,[8] but at least four polymorphs have been reported, in which the α-phase, obtained from solution, has a herringbone structure with a very large dihedral angle of 124°,[9a] whereas the β-phase, obtained again from solution, takes another herringbone structure with small $\theta = 51°$,[9b] and one more different herringbone phase obtained from sublimation has small $\theta = 58°$.[9c] We have recently reported t-butyl-substituted DBTTF with a herringbone structure of $\theta = 41°$.[10] Benzothienobenzothiophene (BTBT, Scheme 1h) derivatives are known owing to excellent mobility even in solution process as well as improved stability.[11] Crystals of alkyl-BTBT (C_n-BTBT for $n = 8$, 10, and 12) and diphenyl-BTBT (DPh-BTBT) have herringbone packing with $\theta = 55$–56 and 42°, respectively.

Gavezzotti and Desiraju have distinguished the above large dihedral-angle phases from the authentic herringbone structure with $\theta = 40$–70°, and designated them as the γ-structure for the $\theta = 90$–110° range and as the β-structure for nearly stacked structures with $\theta > 150°$.[12] It is customary in this work that the dihedral angles are always given in the $\theta < 90°$ range. Accordingly, the supplementary angles are afforded for $\theta > 90°$, so that the β- and γ-structures are respectively reported to be $\theta = 0$–30° and $\theta = 70$–90°. In contrast, we chose the lattice so as to make the intermolecular interactions $c1$ and $c2$ between the parallel molecules always in the vertical directions (Figure 1). From this, we can treat the structures with $\theta > 90°$ continuously from the authentic herringbone structures with $\theta < 90°$ by rotating the molecules. In this definition, the shorter lattice is vertical for (f)–(h), but horizontal for others.

In organic charge-transfer salts and superconductors based on bis(ethylenedithio)tetrathiafulvalene (BEDT-TTF), the herringbone structure is referred to as the θ-phase.[13] There are many θ-salts with different anions, and the dihedral angle varies in a considerable range from 100 to 130°.[14] At the

Published on the web October 6, 2011; doi:10.1246/bcsj.20110176

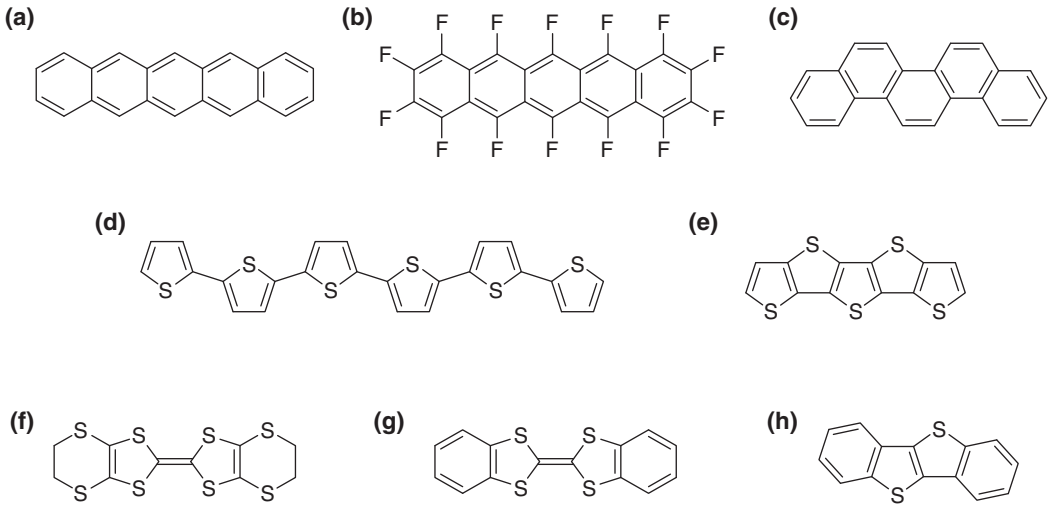

Scheme 1. Molecular structures of (a) pentacene, (b) perfluoropentacene, (c) picene, (d) 6T, (e) f-5T, (f) BEDT-TTF, (g) DBTTF, and (h) BTBT.

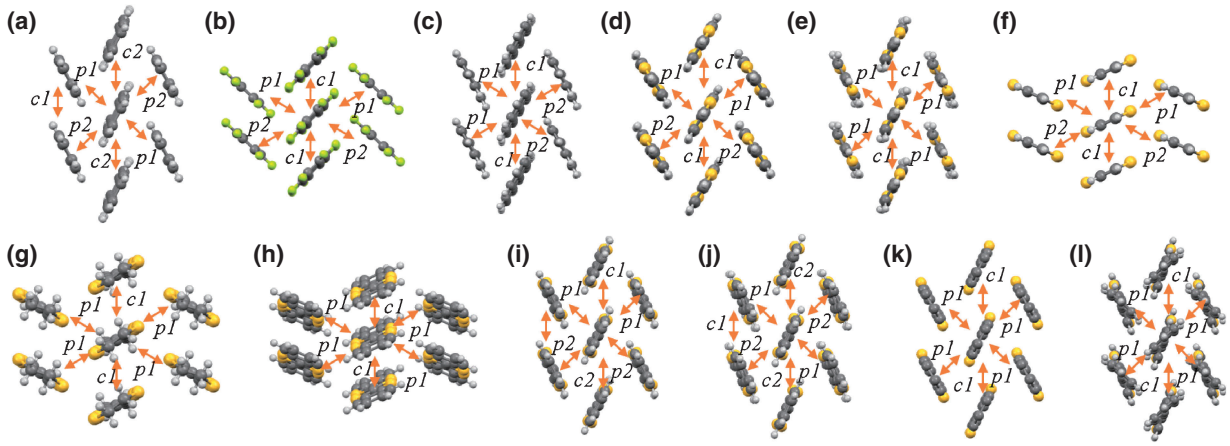

Figure 1. Definition of transfer integrals in the actual crystals of (a) pentacene, (b) perfluoropentacene, (c) picene, (d) 6T/LT phase, (e) 6T/HT phase, (f) f-5T, (g) θ-(BEDT-TTF)$_2$TlCo(SCN)$_4$, (h) DBTTF/α-phase, (i) DBTTF/β-phase, (j) DBTTF/triclinic phase, (k) C_{12}-BTBT (alkyl chains are omitted for clarity), and (l) DPh-BTBT.

same time, the bandwidth changes considerably, and the metal–insulator transition temperature rises from liquid helium temperatures to nearly room temperature. This is known as the universal phase diagram of the θ-phase.[13] For the θ-phase BEDT-TTF, we have calculated the transfer integrals when θ is changed,[14] and revealed that the diagonal transfer integral designated as $p1$ in Figure 1 largely decreases when θ increases. Therefore, θ dependence of the bandwidth is the origin of the universal phase diagram.

Here we investigate dihedral angle dependence of transfer integrals for other organic semiconductors, including pentacene, perfluoropentacene, picene, sexithiophene (6T), pentathienoacene (f-5T), BEDT-TTF, DBTTF, and BTBT. Although the HOMO bands of the BEDT-TTF charge-transfer salts are partially filled and the HOMO bands of organic semiconductors are entirely filled, the transfer integrals are treated in the same framework. Band structures of the herringbone structure have been investigated by many research groups particularly for pentacene[15] and oligothiophenes.[16] Recently, conduction of organic semiconductors is discussed by the hopping model considering the reorganization energy.[17] Here we demonstrate the geometry dependence of the molecular orbital overlap in these organic semiconductors, which is essentially different from BEDT-TTF, and discuss the requirements to realize preferable carrier transport in these materials. Since the molecular orbital overlap of these molecules is much more sensitive to the displacement along the molecular long axis (D) than BEDT-TTF, the D dependence is also investigated.[18] Then we discuss two-dimensional maps of transfer integrals with respect to θ and D, from which we can extract characteristics of each molecule.

Computational Methods

The molecular orbitals (MO) are calculated by Gaussian 09 program at B3LYP/6-31G(d,p) level (Figure 2).[19] The transfer integrals in the actual crystal geometry are calculated by the extended Hückel method.[13b] The atomic orbitals are the same as the standard ones,[14] and sulfur atoms include 3d orbitals. For pentacene, four polymorphs are reported, all of which are slightly different herringbone structure, and the difference of

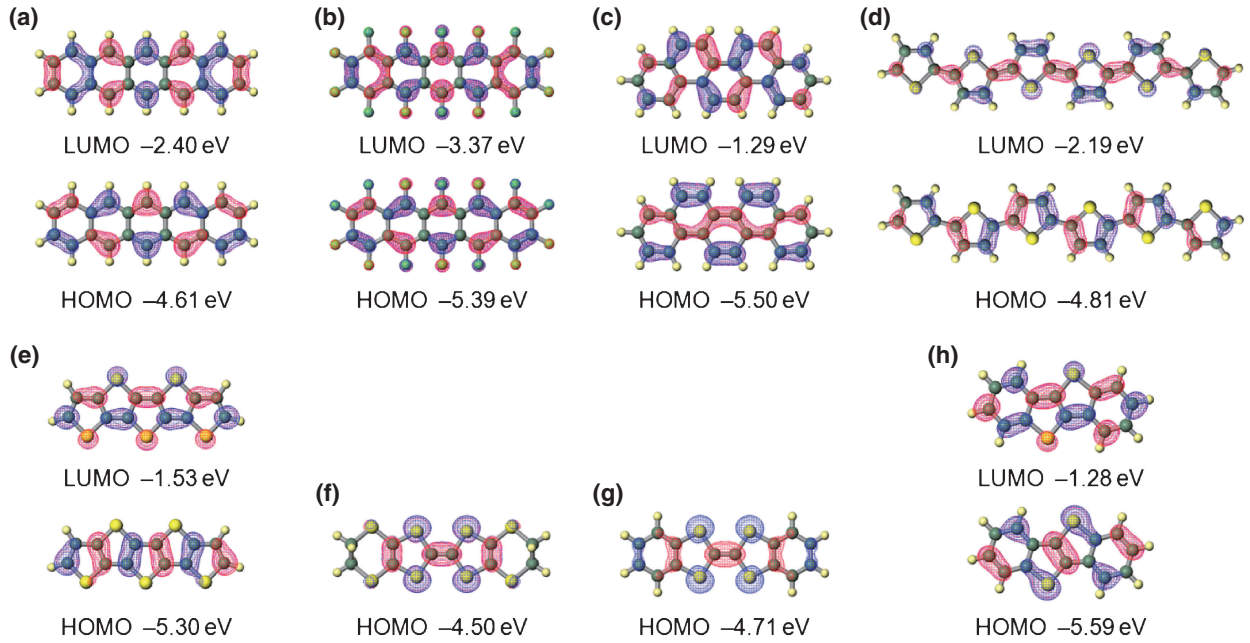

Figure 2. Frontier orbitals of (a) pentacene, (b) perfluoropentacene, (c) picene, (d) 6T, (e) f-5T, (f) BEDT-TTF, (g) DBTTF, and (h) BTBT.

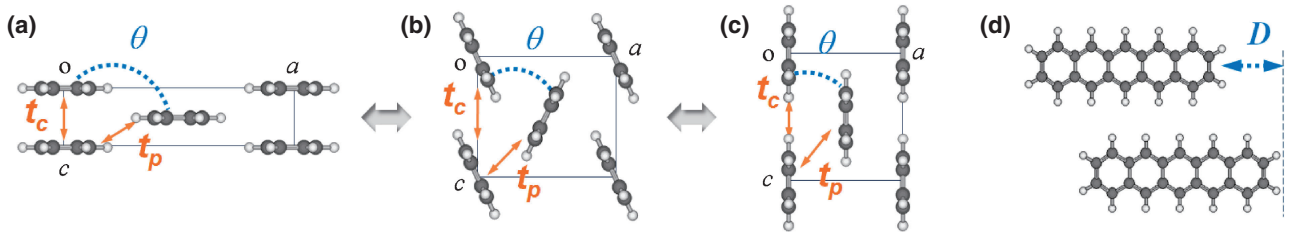

Figure 3. Molecular arrangement at the time of molecular rotation. Starting from (a) the stacking structure at the dihedral angle of $\theta = 180°$, (b) the molecules are rotated up to (c) the vertical molecular arrangement at $\theta = 0°$. (d) Displacement D along the molecular long axis.

the band structure have been discussed.[15c–15f] We mainly discuss the single-crystal phase (Polymorph I) because the detailed structural parameters are available.[2] In order to investigate global geometric dependence of the intermolecular interaction, the transfer integrals are estimated by continuously changing the molecular geometry as shown in Figure 3. The vertical direction is taken as the c axis, and the horizontal intercolumnar direction is called the a axis. In the herringbone structure, there are two kinds of transfer integrals; the diagonal one is designated as t_p, and the vertical one is called t_c. Depending on the crystal symmetry, there are respectively two kinds of $p1/p2$ and $c1/c2$. Atomic coordinates of these molecules are optimized by DFT calculations using the B3LYP functional and 6-31G(d,p) basis set implemented by Gaussian 09 software package. Then one molecule is placed on the corner of the unit cell, and another molecule is located on the center. The $\theta = 180°$ geometry is a simple stacking geometry, where all molecular planes are horizontal (Figure 3a). Here, the lattice constant c is assumed to be 3.4 Å, which is the usual interplanar distance of aromatic molecules. The horizontal a axis is determined from a sum of the van der Waals distance and twice the molecular width. At $\theta = 0°$ all molecules are vertical and parallel to each other again (Figure 3c), where the a axis is twice 3.4 Å, and the c axis is the sum of the molecular width and the van der Waals distance. Then each molecule is rotated around the molecular long axis (Figure 3b) by approximately keeping the van der Waals contacts, in which the lattice constants are linearly changed with respect to $\cos\theta$. This is because in case of the θ-salts of BEDT-TTF, a good linear relation holds between the lattice constants and $\cos\theta$.[14] The actual crystal has a definite θ and has the corresponding actual lattice constants. We have used the lattice constants at $\theta = 180$ and 0° to obtain the linear relation to $\cos\theta$ (Table S1), and confirmed by using the actual crystals. In the calculation, t_c is for a pair of parallel molecules, changes from a stacking arrangement at $\theta = 180°$ to a side-by-side arrangement at $\theta = 0°$. Accordingly, this is approximately equivalent to the parallel rotation reported in Ref. 14, by converting $\phi = \theta/2$, where ϕ is an angle of intermolecular vector measured from the molecular plane.

Overlap integrals between the molecular pairs, S_p and S_c, are calculated using the extended Hückel method.[20] There is another widely adopted way to estimate transfer integrals, where MO calculation of a molecular pair is carried out, and the transfer integrals are evaluated from the level splitting. In this calculation, zero transfer integral does not appear because

Table 1. Transfer Integrals Calculated for the Actual Crystal Geometry

Compound	θ/°	Transfer integrals/meV				Bandwidth /meV	Ref.
		$p1$	$p2$	$c1$	$c2$		
(a) Pentacene	53	−14	24	−2	16	188	2
(b) Perfluoropentacene[a)]	89	0	0	−128	—	512	6
(c) Picene	58	21	30	31	—	266	4
(d) Sexithiophene (6T)/LT	62	0	13	−6	—	76	5a
(e) Sexithiophene (6T)/HT	53	−24	—	2	—	200	5b
(f) Pentathienoacene (f-5T)	130	1	0	18	—	76	7
(g) θ-(BEDT-TTF)$_2$TlCo(SCN)$_4$	119	−96	—	−43	—	940	13b
(h) DBTTF/α-phase	132	12	—	29	—	212	10
(i) DBTTF/β-phase	52	−3	6	−3	12	66	9b
(j) DBTTF/triclinic phase	58	12	−23	−13	−6	178	9c
(k) C_{12}-BTBT	55	−21	—	−32	—	296	11b
(l) DPh-BTBT	42	57	—	51	—	660	11a

a) For LUMO.

the molecular orbitals are renormalized for the respective pair. However, since we want to know the symmetry dependence more explicitly, we adopt the frozen orbital approximation, in which the overlap integrals are calculated from the MO of the single molecule. Subsequently, transfer integrals, t_p and t_c, are estimated by $t = E \times S$, where E is the energy of the MO, and is assumed to be -10 eV. Overlap integrals are also calculated by changing the displacement along the molecular long axis, D (Figure 3d). Thus the overlap integrals are plotted with respect to θ and D on a two-dimensional (2D) plane.

Results and Discussion

Transfer Integrals in the Actual Crystals. Transfer integrals calculated from the actual crystal geometry are shown in Figure 1 and Table 1. The atomic coordinates are taken from the reported X-ray structures, and the HOMO is evaluated from the extended Hückel method,[13b] whereas LUMO is used for perfluoropentacene.

It is obvious from Figure 1 that the usual herringbone structure has dihedral angles around 60°, but (f)–(h) show exceptionally large dihedral angles of 120–130°. Perfluoropentacene in (b) exhibits an intermediate value of 89°. Generally speaking, in the former compounds with small dihedral angles, t_p is approximately equal to t_c, or sometimes larger than t_c. Since t_p is a diagonal interaction and constructs a 2D network, 2D conduction is expected. It should be noted that $p1$ and $p2$ are equivalent from the crystal symmetry in 6T/HT, θ-phase BEDT-TTF, β-phase DBTTF, and BTBT derivatives. In this case, the bandwidth is evaluated from $W = 8t_p + 4t_c$ (Table 1).[14a] Contrarily, in compounds with large dihedral angles such as f-5T and β-phase DBTTF, t_c is dominant, and relatively one-dimensional (1D) conduction is expected. Notably, polymorphs of DBTTF exhibit 2D and 1D conduction depending on the dihedral angles. This however, does not apply to BEDT-TTF; θ-(BEDT-TTF)$_2$TlCo(SCN)$_4$ provides large t_p in spite of the large dihedral angle.[13b]

Maps of Transfer Integrals. Figure 4 shows mapping calculations of transfer integrals plotted with respect to θ and D. Positive transfer integral regions are designated in green, and negative regions are red, but the absolute magnitude is important to make an energy band. The map sometimes crosses zero reflecting the orbital symmetry. Although this is not considered too seriously, because the renormalization of MO gives rise to finite overlap, the zero crossing region is generally expected to afford small transfer integrals. The circles indicate the geometry of the actual crystals discussed in the previous section.

For the pentacene HOMO, t_p takes a maximum at $\theta = 0°$ and decreases monotonously to large θ. This large maximum is close to the stacking arrangement, though the molecules are slipped along the molecular short axis (Figure 3c). t_c has a maximum at $\theta = 180°$ again because this exactly corresponds to the stacking arrangement. The maps of transfer integrals in pentacene demonstrate that only the stacking arrangement is overwhelming. This comes from the molecular structure of pentacene, in which the intermolecular π–π interaction at the side position is blocked by the hydrogen atoms. The map of t_c, however, crosses zero around $\theta = 130°$, and forms a second small peak around $\theta = 90°$. The zero crossing is associated with the long straight node at the molecular center parallel to the molecular long axis (Figure 2a). In general, when the number of nodes is n, the map has $n + 1$ peaks. In this connection, it is noteworthy that t_c of the LUMO does not show zero crossing (Figure 4a), because the LUMO does not have such a long node (Figure 2a). On the contrary, when D is scanned, both t_p and t_c cross zero several times. The periodicity is about 2.8 Å, corresponding to the size of an aromatic ring. This is related to the vertical nodes along the molecular short axis (Figure 2a). Both HOMO and LUMO have this kind of vertical node, and show "D-modulation." At $\theta = 53°$ and $D = 1.8$ Å in the actual bulk crystal, t_p and t_c are reasonably large. These values are by one order of magnitude smaller than the stacking geometry at $\theta = 180$ and 0°, but the balanced t_p and t_c construct the 2D network. This is the reason that the herringbone structure is generally believed to be a 2D structure. The thin-film phases are different from the bulk crystal phase, but are basically the herringbone structure as well.[15c–15h] The D values of the bulk crystal are 0.4 and 1.9 Å for $p1$ and $p2$, whereas these values are 0.1 and 0.3 Å for the thin film phase (Figure 4a).[15f] Accordingly, the thin film phase is expected to be more perfectly two-dimensional. The bandwidth of pentacene is estimated to be 188 meV (Table 1) in agreement with the previous calculations.[15] Perfluoropentacene is located at

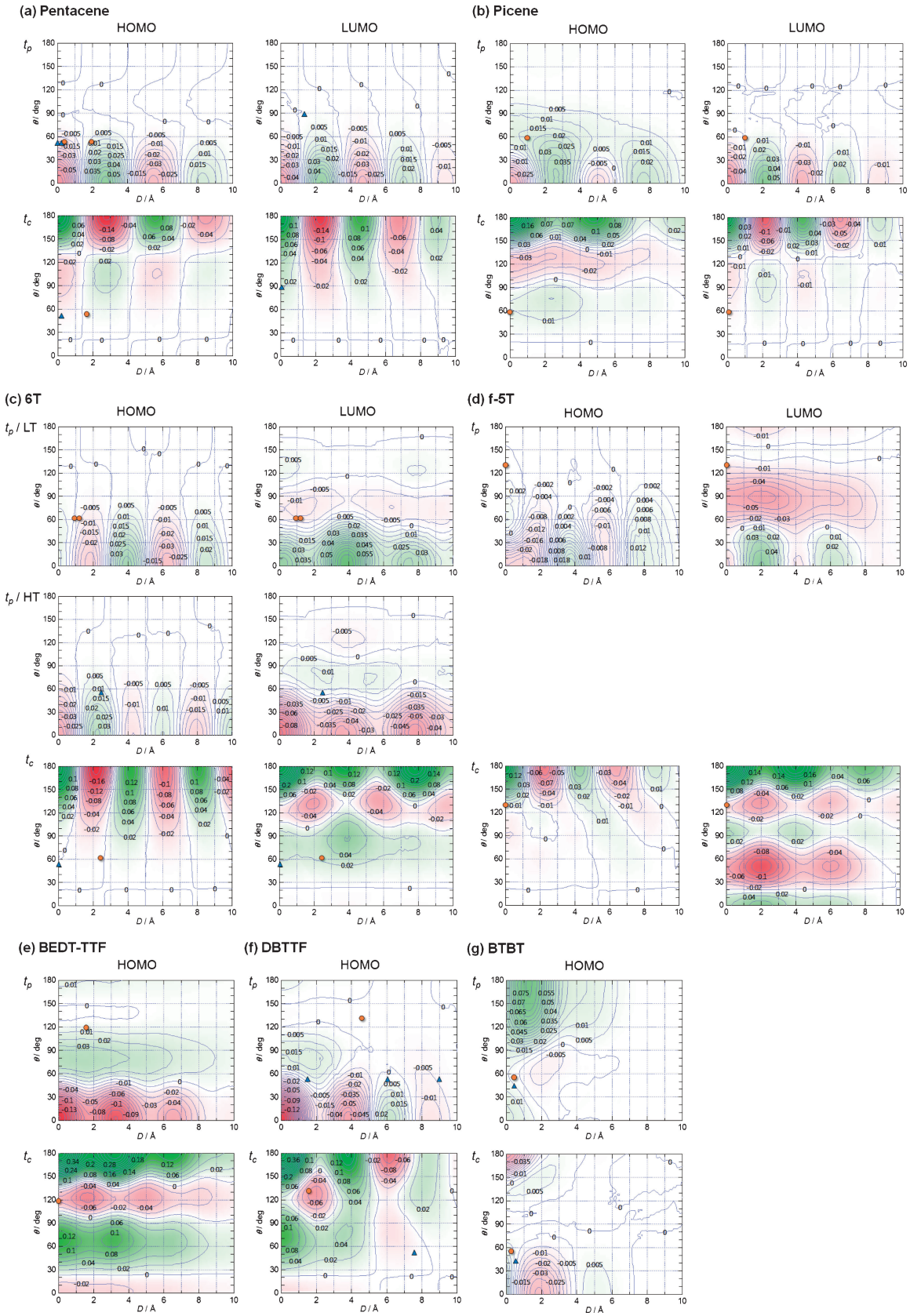

Figure 4. 2D map of transfer integrals, t_p and t_c, with respect to θ and D for (a) pentacene (b) picene, (c) 6T, (d) f-5T, (e) BEDT-TTF, (f) DBTTF, and (g) BTBT. Circles and triangles are geometries in the actual crystals and the polymorphs. (a) Circles are for the bulk crystal, and triangles are for the thin film phase. Circles in LUMO of (a) are for perfluoropentacene. In (g), circles are for C_{12}-BTBT, and triangles are for DPh-BTBT.

$\theta = 89°$ in the actual crystal, where t_p is practically zero and only t_c has meaningful magnitude, leading to 1D interaction. This agrees with the calculation from the actual crystal geometry (Table 1), and the previous band calculations.[21] The bandwidth (512 meV) is, however, significantly larger than pentacene (188 meV). This example demonstrates that dimensionality of the herringbone packing is sensitive to the dihedral angle.

For picene, the HOMO has two long transverse nodes along the molecular long axis (Figure 2c). As a result, t_c changes sign twice when θ is scanned (Figure 4b), and the map of t_c shows "θ-modulation" with peaks at $\theta = 180$, 120, and 60°. Interestingly, the map of t_p still shows D-modulation. This difference comes from the inclined molecular arrangement in t_p, which obscures the influence of the long nodes, whereas the parallel molecular planes in t_c suffer from a stricter effect of the long nodes. Magnitudes of t_p and t_c are comparable in the actual crystal geometry, leading to 2D energy band with a bandwidth of 266 meV.

Oligothiophenes are represented by sexithiophene (6T). 6T shows two phases depending on the temperature.[5] One molecule is crystallographically independent in the low-temperature (LT) phase, and there are twofold screw axes along the horizontal axis (the a axis in Figure 3). The molecule in the high-temperature (HT) phase is located on an inversion center, and twofold screw axes are parallel to the vertical axis (the c axis in Figure 3). Therefore t_c is the same in both phases. The maps of the HOMO in the LT phase show a pattern similar to pentacene. The maps are dominated by the D-modulation, and monotonously decrease from the stacking geometry at $\theta = 0°$ for t_p and $\theta = 180°$ for t_c. 2D conduction is realized by t_p, which has comparable magnitude to pentacene (Table 1). The HT phase provides basically similar maps to the LT phase (in the middle of Figure 4c). The HT phase has a smaller dihedral angle (53°) than the LT phase (62°). Accordingly, it is expected from the maps that the HT phase has larger t_p. This is in agreement with the individual calculations in Table 1. The resulting band width of 200 meV is a little smaller than previous reports (400 meV),[16] but it is reasonable that oligothiophene and pentacene have approximately similar bandwidths.

In the maps of the LUMO of 6T (Figure 4c), the D-modulation is largely replaced by the θ-modulation, and the amplitude becomes relatively large. This comes from the population on the sulfur atoms, though the HOMO does not have population on the sulfur atoms (Figure 2d). If electron transport is realized in an oligothiophene, the bandwidth is expected to be larger than the hole transport. Actually, electron transport has been observed in some oligothiophenes with fluorinated alkyl chains.[22]

As an example of fused-oligothiophenes, pentathienoacene (f-5T) is investigated. As depicted in Figure 2e, the MO symmetry of the respective thiophene unit is similar to that of the oligothiophene (Figure 2d). Consequently, the mapping patterns are very close to those of 6T, where the D-modulation is predominant in the HOMO, and θ-modulation appears in the LUMO. In particular, the θ-modulation in the LUMO is remarkable, and relatively large side interactions are expected. These features are consistent with previous calculations.[23]

As we have previously reported,[14] t_c of BEDT-TTF shows pronounced θ-modulation (Figure 4e). This is associated with the entirely symmetric HOMO, where all sulfur atoms have the same phase (Figure 2f). The peaks of t_c appear around 0, 60, 120, and 180°, which is basically identical to our previous results of parallel rotation if we take $\phi = \theta/2$.[14] BEDT-TTF affords very large transfer integrals due to the multiple sulfur atoms aligned at the molecular side, and it is particularly characteristic that considerable interaction appears even at the side position around $\theta = 0°$. t_p also mainly exhibits θ-modulation, and shows a peak around 90°. The upper slope of this peak in the region of $\theta = 90$–130° is the origin of the universal phase diagram of the θ-phase.[14] It should be noted that BEDT-TTF provides much larger bandwidth of 940 meV than other organic semiconductors (Table 1).

Interestingly, DBTTF shows considerably different maps from BEDT-TTF in spite of the same core skeleton (Figure 4f), and the map looks like a hybrid of θ- and D-modulations. This is because the MO symmetry of the benzene rings plays an important role in the large D region, and the map shows a hybridized feature of pentacene and BEDT-TTF. As another consequence, t_p for large θ is not as large as BEDT-TTF around the actual $\theta = 132°$ of the α-phase DBTTF, so that the α-phase DBTTF is expected to be relatively 1D. Molecular long axes of a DBTTF pair for t_p in the α-phase are, however, not strictly parallel to each other, but twisted about 12°. Accordingly, the transfer integrals in Table 1 are a little different from the values estimated from the maps, and the α-phase DBTTF is not highly 1D. Among many polymorphs of DBTTF, the β-phase is a normal herringbone structure with a dihedral angle of 52°, where t_p is larger than t_c, leading to 2D interaction (Table 1). The bandwidth of β-phase (66 meV) is, however, smaller than 212 meV of the α-phase and 178 meV of the triclinic phase. DBTTF is repeatedly investigated as an OFET material, where the highest reported mobility is $1\,cm^2\,V^{-1}\,s^{-1}$ in a single crystal,[8a] but DBTTF sometimes shows much lower performance,[8c,8d] probably due to the polymorphic modifications. It has been recently discussed that the highest value comes from the α-phase.[24] In our calculation, the α-phase affords the largest bandwidth (Table 1h).

BTBT derivatives are a material which shows extremely high OFET performance.[11] The calculation affords relatively large bandwidths both for C_{12}-BEBT and DPh-BTBT (Table 1). This result is in accordance with the calculation reported in Ref. 25. The maps are however, much different from other organic semiconductors (Figure 4g). This is again a hybrid of θ- and D-modulations, but it is noteworthy that t_p has a significant magnitude over the wide range of θ values, and particularly even at the side ($\theta = 180°$) position. This is related to the significant HOMO population on the sulfur atoms as well as the absence of the long straight node (Figure 2h). The MO symmetry agrees with previous MO calculation.[26] BTBT has a single sulfur atom on each side, but it works similarly to two in-phase side sulfur atoms of TTF. These sulfur atoms play an important role in enhancing the side interaction. It has been pointed out that the phene structure of BTBT, similarly to chrysene, gives rise to the low HOMO level and is an origin of stable transistor performance.[26] A series of benzothiophenes have been developed recently, and the variations of the transistor properties have been

investigated.[25] Judging from the reported molecular orbitals, large MO population on sulfur is not common to the phene structure, but some straight benzothiophenes show this property. Differently from TTF, the transfer integrals of BTBT decay rapidly at large D (Figure 4g). This decay is not so large for DPh-BTBT, and this leads to the relatively large bandwidth of DPh-BTBT in Table 1.

Discussion. The 2D plot of the transfer integrals are roughly classified to two patterns: D-modulation and θ-modulation. The modulation pattern depends on the symmetry of the MO; the vertical nodes along the molecular short axis afford the D-modulation, whose periodicity is determined by the ring size. The θ-modulation is related to the nodes along the molecular long axis. The θ-modulation affords several peaks in the middle θ range and provides an opportunity to realize large transfer integrals in the actual system. The magnitude of the transfer integrals is enhanced by sulfur atoms because the extended atomic orbital affords large intermolecular interactions.

The dihedral angle is an important factor to determine the dimensionality in the compounds showing the D-modulation, because both t_p and t_c transfer integrals are monotonously decreasing functions starting from the maxima at the π-stacking. This does not apply to the compounds showing θ-modulation, because many peaks appear in the middle θ range. Many traditional OFET materials such as pentacene and 6T as well as f-5T are recognized as D-modulation materials, so the dihedral angle is crucial to determine the dimensionality and magnitude of intermolecular interactions. Materials with θ-modulation are not sensitive to the dihedral angle in general, and usually provide greater interactions at the side position. BEDT-TTF is a well-known example that shows 2D interaction, but BTBT is another example that exhibits excellent 2D interaction. It should be emphasized that these differences stem from the MO symmetry, and originally comes from the molecular structure.

Summary

We have investigated the angular dependence of transfer integrals based on the MO calculations by scanning the global geometry. It is an important point to consider the $\theta > 90°$ region, which is discussed continuously from the authentic herringbone structures. The largely different qualitative patterns reported here is valid even when we carry out more elaborated calculations. In the authentic herringbone structures such as pentacene and oligothiophenes, small θ is necessary to realize 2D transport, but different MO symmetry is required to achieve 2D conduction in large θ materials. f-5T is not much different from oligothiophenes, whereas BTBT fulfills the latter condition, which rivals the side interactions of TTF.

This work was supported by the global COE program "Education and Research Center for Emergence of New Molecular Chemistry" from Ministry of Education, Culture, Sports, Science and Technology of Japan.

Supporting Information

The linear relations used for obtaining lattice constants from $\cos\theta$. This material is available free of charge on the web at http://www.csj.jp/journals/bcsj/.

References

1 *Organic Electronics*, ed. by H. Klauk, Wiley, Weinheim, **2006**.

2 a) R. B. Campbell, J. M. Robertson, J. Trotter, *Acta Crystallogr.* **1961**, *14*, 705. b) C. C. Mattheus, A. B. Dros, J. Baas, A. Meetsma, J. L. de Boer, T. T. M. Palstra, *Acta Crystallogr., Sect. C* **2001**, *57*, 939.

3 H. Okamoto, N. Kawasaki, Y. Kaji, Y. Kubozono, A. Fujikawa, M. Yamaji, *J. Am. Chem. Soc.* **2008**, *130*, 10470.

4 A. De, R. Ghosh, S. Roychowdhury, P. Roychowdhury, *Acta Crystallogr., Sect. C* **1985**, *41*, 907.

5 a) G. Horowitz, B. Bachet, A. Yassar, P. Lang, F. Demanze, J.-L. Fave, F. Garnier, *Chem. Mater.* **1995**, *7*, 1337. b) T. Siegrist, R. M. Fleming, R. C. Haddon, R. A. Laudise, A. J. Lovinger, H. E. Katz, P. Bridenbaugh, D. D. Davis, *J. Mater. Res.* **1995**, *10*, 2170.

6 Y. Sakamoto, T. Suzuki, M. Kobayashi, Y. Gao, Y. Fukai, Y. Inoue, F. Sato, S. Tokito, *J. Am. Chem. Soc.* **2004**, *126*, 8138.

7 X. Zhang, A. P. Côté, A. J. Matzger, *J. Am. Chem. Soc.* **2005**, *127*, 10502.

8 a) M. Mas-Torrent, P. Hadley, S. T. Bromley, N. Crivillers, J. Veciana, C. Rovira, *Appl. Phys. Lett.* **2005**, *86*, 012110. b) Naraso, J. Nishida, S. Ando, J. Yamaguchi, K. Itaka, H. Koinuma, H. Tada, S. Tokito, Y. Yamashita, *J. Am. Chem. Soc.* **2005**, *127*, 10142. c) K. Shibata, K. Ishikawa, H. Takezoe, H. Wada, T. Mori, *Appl. Phys. Lett.* **2008**, *92*, 023305. d) T. Yamada, T. Hasegawa, M. Hiraoka, H. Matsui, Y. Tokura, G. Saito, *Appl. Phys. Lett.* **2008**, *92*, 233306. e) B. Noda, H. Wada, K. Shibata, T. Yoshino, M. Katsuhara, I. Aoyagi, T. Mori, T. Taguchi, T. Kambayashi, K. Ishikawa, H. Takezoe, *Nanotechnology* **2007**, *18*, 424009.

9 a) T. J. Emge, F. M. Wiygul, J. S. Chappell, A. N. Bloch, J. P. Ferraris, D. O. Cowan, T. J. Kistenmacher, *Mol. Cryst. Liq. Cryst.* **1982**, *87*, 137. b) A. Brillante, I. Bilotti, R. G. D. Valle, E. Venuti, S. Milita, C. Dionigi, F. Borgatti, A. N. Lazar, F. Biscarini, M. Mas-Torrent, N. S. Oxtoby, N. Crivillers, J. Veciana, C. Rovira, M. Leufgen, G. Schmidt, L. W. Molenkamp, *CrystEngComm* **2008**, *10*, 1899. c) M. Mamada, Y. Yamashita, *Acta Crystallogr., Sect. E* **2009**, *65*, o2083.

10 J. Nagakubo, M. Ashizawa, T. Kawamoto, A. Tanioka, T. Mori, *Phys. Chem. Chem. Phys.* **2011**, *13*, 14370.

11 a) K. Takimiya, H. Ebata, K. Sakamoto, T. Izawa, T. Otsubo, Y. Kunugi, *J. Am. Chem. Soc.* **2006**, *128*, 12604. b) H. Ebata, T. Izawa, E. Miyazaki, K. Takimiya, M. Ikeda, H. Kuwabara, T. Yui, *J. Am. Chem. Soc.* **2007**, *129*, 15732. c) T. Izawa, E. Miyazaki, K. Takimiya, *Adv. Mater.* **2008**, *20*, 3388. d) C. Liu, T. Minari, X. Lu, A. Kumatani, K. Takimiya, K. Tsukagoshi, *Adv. Mater.* **2011**, *23*, 523. e) J. Soeda, Y. Hirose, M. Yamagishi, A. Nakao, T. Uemura, K. Nakayama, M. Uno, Y. Nakazawa, K. Takimiya, J. Takeya, *Adv. Mater.* **2011**, *23*, 3309.

12 a) G. R. Desiraju, A. J. Gavezzotti, *J. Chem. Soc. Chem. Commun.* **1989**, 621. b) G. R. Desiraju, A. Gavezzotti, *Acta Crystallogr., Sect. B* **1989**, *45*, 473.

13 a) H. Mori, S. Tanaka, T. Mori, *Phys. Rev. B* **1998**, *57*, 12023. b) H. Mori, S. Tanaka, T. Mori, A. Kobayashi, H. Kobayashi, *Bull. Chem. Soc. Jpn.* **1998**, *71*, 797.

14 a) T. Mori, H. Mori, S. Tanaka, *Bull. Chem. Soc. Jpn.* **1999**, *72*, 179. b) T. Mori, *Bull. Chem. Soc. Jpn.* **1998**, *71*, 2509.

15 a) R. C. Haddon, X. Chi, M. E. Itkis, J. E. Anthony, D. L. Eaton, T. Siegrist, C. C. Mattheus, T. T. M. Palstra, *J. Phys. Chem. B* **2002**, *106*, 8288. b) Y. C. Cheng, R. J. Silbey, D. A. da Silva Filho, J. P. Calbert, J. Cornil, J. L. Brédas, *J. Chem. Phys.* **2003**,

118, 3764. c) C. C. Mattheus, G. A. de Wijs, R. A. de Groot, T. T. M. Palstra, *J. Am. Chem. Soc.* **2003**, *125*, 6323. d) C. C. Mattheus, A. B. Dros, J. Baas, G. T. Oostergetel, A. Meetsma, J. L. de Boer, T. T. M. Palstra, *Synth. Met.* **2003**, *138*, 475. e) A. Troisi, G. Orlandi, *J. Phys. Chem. B* **2005**, *109*, 1849. f) H. Yoshida, N. Sato, *Phys. Rev. B* **2008**, *77*, 235205. g) H. Yoshida, N. Sato, *Appl. Phys. Lett.* **2006**, *89*, 101919. h) H. Yoshida, K. Inaba, N. Sato, *Appl. Phys. Lett.* **2007**, *90*, 181930.

16 a) R. C. Haddon, T. Siegrist, R. M. Fleming, P. M. Bridenbaugh, R. A. Laudise, *J. Mater. Chem.* **1995**, *5*, 1719. b) P. Hermet, J.-L. Bantignies, A. Rahmani, J.-L. Sauvajol, M. R. Johnson, *J. Phys. Chem. A* **2005**, *109*, 4202. c) J. L. Brédas, R. L. Elsenbaumer, R. R. Chance, R. Silbey, *J. Chem. Phys.* **1983**, *78*, 5656.

17 a) E. F. Valeev, V. Coropceanu, D. A. da Silva Filho, S. Salman, J.-L. Brédas, *J. Am. Chem. Soc.* **2006**, *128*, 9882. b) F. Castet, P. Aurel, A. Fritsch, L. Ducasse, D. Liotard, M. Linares, J. Cornil, D. Beljonne, *Phys. Rev. B* **2008**, *77*, 115210. c) J. Idé, R. Méreau, L. Ducasse, F. Castet, Y. Olivier, N. Martinelli, J. Cornil, D. Beljonne, *J. Phys. Chem. B* **2011**, *115*, 5593.

18 a) J. L. Brédas, J. P. Calbert, D. A. da Silva, J. Cornil, *Proc. Natl. Acad. Sci. U.S.A.* **2002**, *99*, 5804. b) O. Kwon, V. Coropceanu, N. E. Gruhn, J. C. Durivage, J. G. Laquindanum, H. E. Katz, J. Cornil, J. L. Brédas, *J. Chem. Phys.* **2004**, *120*, 8186.

19 M. J. Frisch, G. W. Trucks, H. B. Schlegel, G. E. Scuseria, M. A. Robb, J. R. Cheeseman, G. Scalmani, V. Barone, B. Mennucci, G. A. Petersson, H. Nakatsuji, M. Caricato, X. Li, H. P. Hratchian, A. F. Izmaylov, J. Bloino, G. Zheng, J. L. Sonnenberg, M. Hada, M. Ehara, K. Toyota, R. Fukuda, J. Hasegawa, M. Ishida, T. Nakajima, Y. Honda, O. Kitao, H. Nakai, T. Vreven, J. A. Montgomery, Jr., J. E. Peralta, F. Ogliaro, M. Bearpark, J. J. Heyd, E. Brothers, K. N. Kudin, V. N. Staroverov, R. Kobayashi, J. Normand, K. Raghavachari, A. Rendell, J. C. Burant, S. S. Iyengar, J. Tomasi, M. Cossi, N. Rega, J. M. Millam, M. Klene, J. E. Knox, J. B. Cross, V. Bakken, C. Adamo, J. Jaramillo, R. Gomperts, R. E. Stratmann, O. Yazyev, A. J. Austin, R. Cammi, C. Pomelli, J. W. Ochterski, R. L. Martin, K. Morokuma, V. G. Zakrzewski, G. A. Voth, P. Salvador, J. J. Dannenberg, S. Dapprich, A. D. Daniels, Ö. Farkas, J. B. Foresman, J. V. Ortiz, J. Cioslowski, D. J. Fox, *Gaussian 09 (Revision B. 01)*, Gaussian, Inc., Wallingford CT, **2009**.

20 T. Mori, A. Kobayashi, Y. Sasaki, H. Kobayashi, G. Saito, H. Inokuchi, *Bull. Chem. Soc. Jpn.* **1984**, *57*, 627.

21 M. C. R. Delgado, K. R. Pigg, D. A. da Silva Filho, N. E. Gruhn, Y. Sakamoto, T. Suzuki, R. M. Osuna, J. Casado, V. Hernández, J. T. L. Navarrete, N. G. Martinelli, J. Cornil, R. S. Sánchez-Carrera, V. Coropceanu, J.-L. Brédas, *J. Am. Chem. Soc.* **2009**, *131*, 1502.

22 a) A. Facchetti, Y. Deng, A. Wang, Y. Koide, H. Sirringhaus, T. J. Marks, R. H. Friend, *Angew. Chem., Int. Ed.* **2000**, *39*, 4547. b) M.-H. Yoon, S. A. DiBenedetto, A. Facchetti, T. J. Marks, *J. Am. Chem. Soc.* **2005**, *127*, 1348. c) A. Facchetti, J. Letizia, M.-H. Yoon, M. Mushrush, H. E. Katz, T. J. Marks, *Chem. Mater.* **2004**, *16*, 4715.

23 E.-G. Kim, V. Coropceanu, N. E. Gruhn, R. S. Sánchez-Carrera, R. Snoeberger, A. J. Matzger, J.-L. Brédas, *J. Am. Chem. Soc.* **2007**, *129*, 13072.

24 M. Mas-Torrent, C. Rovira, *Chem. Rev.* **2011**, *111*, 4833.

25 a) S. Shinamura, I. Osaka, E. Miyazaki, A. Nakao, M. Yamagishi, J. Takeya, K. Takimiya, *J. Am. Chem. Soc.* **2011**, *133*, 5024. b) I. Osaka, T. Abe, S. Shinamura, K. Takimiya, *J. Am. Chem. Soc.* **2011**, *133*, 6852.

26 K. Takimiya, T. Yamamoto, H. Ebata, T. Izawa, *Sci. Technol. Adv. Mater.* **2007**, *8*, 273.